OPERATIONAL CHALLENGES AND RESULTS FROM AN EXPERIMENTAL ONE KILOWATT ORGANIC RANKINE CYCLE

Richard Wijninckx[1], Susan Krumdieck[1]

[1]*Department of Mechanical Engineering, University of Canterbury, Private Bag 4800, Christchurch 8041, New Zealand*

[1]richard.wijninckx@pg.canterbury.ac.nz

[1]Susan.krumdieck@canterbury.ac.nz

Keywords: *Experimental Organic Rankine Cycle, ORC, Scroll expander, System Performance, Power generation from waste heat, Zeotropic mixture, M1.*

ABSTRACT

Organic Rankine Cycle (ORC) systems are capable of utilising low-enthalpy heat sources to generate power. For the performance engineering of ORC systems, it is important to understand process parameters and component behaviour. To maximise performance, modelling of the plant thermodynamics must be coupled with data analysis to develop diagnostic procedures, find optimal operating points, and diagnose problems to schedule the most cost effective maintenance. An existing ORC system at the University of Canterbury has been upgraded from a previous iteration to assist in furthering our knowledge of ORC system design and construction.

This paper presents experimental results from running a 1 kW ORC system using HFC-M1 refrigerant, a zeotropic mixture of R245fa and R365mfc, as the working fluid under a wide range of operating conditions. Hot exhaust combustion products from a 30kW CapstoneTM Gas Turbine are used as the heat source and heat is transferred via a thermal oil loop to the working fluid through a plate heat exchanger. A scroll expander magnetically coupled to an AC generator is used for work extraction and energy conversion. Trials focused on off-design performance, and investigated the effect of varying the refrigerant volume ratio on system performance. Trials were prematurely ended by bearing failure in the expander. A comparative study was performed between the system actual performance and the theoretical performance to evaluate the degree of impact of the operational issues on the system performance. The unit was disassembled to evaluate the component compatibility and assess functionality over the operation. The system mass was not conserved during the operation due to leakage, contributing to the overall deterioration in system performance over time.

1. INTRODUCTION

1.1 ORC background

Rankine cycle systems are commonly used to generate power from thermal sources. An organic Rankine cycle system utilises a refrigerant as the working fluid to generate power from low temperature heat sources at a higher efficiency than a traditional steam system. A small laboratory scale 1kW ORC system was built at the University of Canterbury to investigate the behaviour of a small scale system (Meyer, Wong, Engel, & Krumdieck, 2013).

1.2 Purpose of experiments

The ORC-B system was constructed in 2013 at the University of Canterbury in order to provide a test bench for refrigerant heat exchange and various expander options.

This configuration was only ever partially tested before critical improvements were identified (Southon & Krumdieck, 2014). With these implemented, this study aimed to thoroughly investigate the systems performance over the available input range. Of particular interest was investigation of the effect of the liquid level charge as a ratio of total system volume (abbreviated to the "Dimensionless Volume Ratio" or DVR) on the performance.

2 EXPERIMENTAL SETUP

2.1 System

The ORC system consists of four separate fluid loops – the exhaust gas heat source, thermal oil transfer, working fluid, and cooling water. Three heat exchangers, two brazed plate and one finned tube type, facilitate heat transfer.

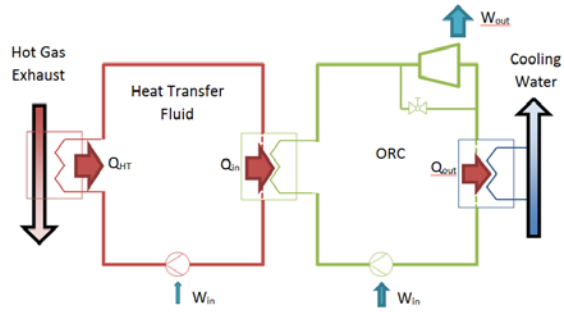

Figure 1: Diagram showing the heat and work flows of the ORC system and thermal oil loop.

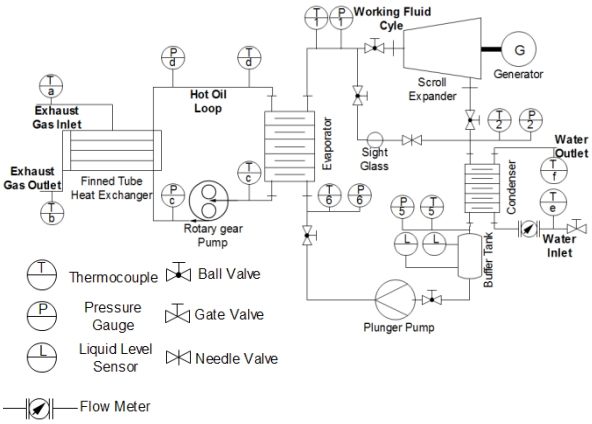

Figure 2: Layout of ORC system. Image produced by Leighton Taylor.

2.2 Heat Source

A 30 kW Capstone Microturbine system serves as the heat source for the ORC. The Capstone system combusts diesel

fuel, and the hot waste gasses from this combustion are passed through a finned tube heat exchanger (FTHE) to heat the thermal oil in the heat transport loop.

The exhaust flow is controlled by setting a desired power output between 0 – 30 kW on the turbine. The flow rate of the gas exhaust products is correlated with this power output setting using manufacturer data (Capstone, 2006). Thermocouples placed inside the gas exhaust stream before and after the FTHE measure the gas temperature drop.

2.3 Heat Transfer system

Due to the nature of the heat source, the temperature at the wall of heat exchanger in the exhaust reaches 280ºC, which would cause thermal decomposition of some refrigerant working fluids intended for testing in the system. Therefore an intermediate oil transfer loop was employed to extract heat to the ORC.

The thermal oil is is CALFLOW^{TM} High Temperature Heat Transfer Fluid (HTF) from PETRO-CANADA. Manufacturer data on the density and heat capacity were used for heat rate calculations. The heat capacity is assumed to be independent of pressure and is given by Equation 1.

$$C_{p,tf} = 3.46 \times T_{tf,m} + 1807.86\ (J/kg) \quad (1)$$

The heat transfer fluid is circulated throughout the thermal oil loop using a gear-type positive displacement pump, controlled by a variable frequency drive. The relationship between pump motor controller speed and the thermal oil flow rate was determined using Equation 2 (Engel, 2013).

$$\dot{V}_{tf} = (0.0103\ L \times n + 0.20\ L/min) \quad (2)$$

Here n is the pump motor controller speed. Oil pump power consumption was assumed to be dominated by motor speed, as there is only a small pressure increase during operation. Power measurements at frequencies within the operating range were taken with a clamp meter, providing a relationship used in efficiency calculations (Equation 3).

$$\dot{W}_{pump,tf} = 1.89 \times n + 95.4\ (W) \quad (3)$$

2.4 Expansion Device

The expander is one of the most critical components in a low-capacity ORC system (Declaye, Quoilin, Guillaume, & Lemort, 2013). In this power range, expander selection is limited. This system makes use of a scroll type expander, rated for 1 kW from AirSquared. The expander was chosen for its fully sealed and oil-free design. A magnetic coupling transfers shaft work to an AC generator, with the resulting generated power recorded with a clamp meter, denoted by $\dot{W}_{gen}$. Generator resistance is provided by light bulbs, able to be switched independently, rated at 100W, 200W, and two at 500W.

2.5 ORC loop

The scroll expander is placed in an ORC system comprised of a plate type evaporator, a plate type condenser, a buffer tank and a working fluid pump. Where practical, sources of heat loss (e.g. evaporator, stainless piping) were insulated with insulation foam, with the exception of the expander.

The evaporator and condenser are 60 and 40 plate heat exchangers, respectively, both designed to transfer 20 kW of heat in operation.

The municipal water supply is passed through the condenser in a once-through cooling system. The flow rate is controlled with a gate valve, and measured with a rotary piston meter.

A custom manufactured 1.8 L buffer tank is located before the pump to allow the system to behave dynamically during start-up and while testing different operating conditions. The tank also ensures that there is always liquid being provided to the pump as vapour can damage the seals in the pump. Two optical sensors indicated the fluid level in the tank.

The working fluid pump is a three-cylinder piston type positive displacement pump controlled by variable frequency drive. The fluid flow rate is measured by an analogue Variable Area Flowmeter calibrated to the working fluid. Working fluid pump power consumption was recorded using a clamp meter.

2.6 Working fluid

The working fluid for the system is a refrigerant called HFC-M1. The fluid consists of a zeotropic mixture of R245fa and R365mfc at 52.8% and 47.2% mole fractions. All state properties of the M1 fluid mixture are calculated using the NIST REFPROP 9.0 fluid property database software (Lemmon, 2013).

2.7 Control and Data Collection

A LABVIEW program created by Alexandre Mugnier is used to control the inputs for the ORC system. The program sorts and records the data obtained from the sensors through a National Instruments DAQ.

2.8 Component summary

Table 1: Key components in 1 kW ORC system.

Component	Type
Evaporator	Brazed 316 SS 60 plate. 6.374 m^2 total surface area.
Condenser	Brazed 316 SS 40 plate. 1.805 m^2 total surface area.
Thermal oil pump	Gear type pump. 11 cc/rev.
Thermal oil pump motor	1.5 HP (1.1 kW). 1 winding.
Working fluid pump	3 cylinder piston pump. 4.81 cc/rev.
Working fluid pump motor	0.5 HP (373 W). 4 poles.
Expander	Scroll type 12 cc/rev. Fixed volume ratio = 3.5.
Generator	AC asynchronous with voltage regulation. 2.4 kW, 240V operation at 50 Hz.
Working fluid	M1 refrigerant. 50.3 wt% R245fa, 49.7 wt% R365mfc.
Heat transfer fluid	High temperature, low visc. HTF oil.
DAQ	National Instruments CompactDAQ.

2.9 Measurement Devices

The measurement devices used to determine fluid properties and generator power output are shown in Table 2. All measurements were sampled at 0.5 Hz and recorded at 2 Hz.

Table 2: Measurement devices

	Quantity	Measurement device / method
Exhaust	Flow rate	Estimated using manufacturer data.
	Temperature	Type-K thermocouples.
	Pressure	Reasonable estimate.
Transfer Fluid	Flow	Gear-pump motor speed
	Temperature	Type-T thermocouples.
	Pressure	Piezoresistive Pressure Transducers
Working Fluid	Flow rate	Variable Area Flowmeter
	Temperature	Type-K thermocouples.
	Pressure	Piezoresistive Pressure Transducers
Cooling Water	Flow	Rotary piston meter.
	Temperature	Type-T thermocouples.
	Pressure	Estimated from municipal.
Power Output	Magnitude & Frequency	Clamp-on power quality meter
	Shaft Speed	Optical transducer

Figure 3: Picture of completed test rig at UC. (Pre-insulation, for clarity of components).

3 EXPERIMENTAL PROCEDURE

3.1 Dimensionless Volume Ratio

Work by Li et al. suggests there is an optimal ratio of refrigerant volume to system volume for a small scale ORC using R245fa, finding optimal performance at a DVR of 0.41 (Li, Zhu, Fu, & Hu, 2015). To investigate this, a DVR range of 0.61-0.21 in five increments was proposed. The ORC system volume was estimated as accurately as possible, and charged with 9.26kg of fluid achieving a DVR of 0.62.

This initial test was designed to ascertain the impacts of the various controllable inputs on system performance. The next step was to select an optimal range and proceed, decreasing the DVR with each trial. However, component failure in the initial trial meant that only one data set was able to be collected with a functioning expander.

3.2 Scroll tests

To ascertain the impact of the controllable inputs on system performance, the system was systematically progressed through its full range of parameters, detailed in Table 3.

Table 3 – Summary of testing inputs

Component	Setting
Capstone Turbine (heat source)	5-25 kW in 5kW steps
Thermal Oil Pump	6, 12, 18 Hz
Working fluid pump	12 – 27.5Hz (Flow rate 0.02 to 0.06 kg/s
Cooling water flow	Inlet valve fully open, flow rate between 0.9 and 1.1 kg/s.
Generator resistance	500W and 1000W
Ambient Temp.	17-20 Degrees Celsius

Towards the end of the trial the expander bearings failed, forcing a different approach to be taken for the remainder of the trials.

3.3 Dimensionless Volume Ratio tests

A needle valve in the bypass loop was used to impose a pressure differential on the system in lieu of an expander, with the aim of achieving the highest possible pressure ratio and observing the mass flow rate required to sustain this.

This was done at three different heat rates for each DVR, which progressed from 0.53 to 0.27 in 5 increments.

3.4 Steady State Definition

Achieving a consistent steady state was a critical factor in examining performance. Data was monitored until the following criteria were met and sustained for 5 minutes:

Temperature probes ± 1ºC

Pressure readings ± 5%

In post processing, appropriate low pass filters were then applied to the data. Following this, a sliding buffer of length equal to 5 minutes parsed the data and returned times where the coefficient of variance of all sensors was under 0.5%, where applicable. These were then used as steady state points in the results.

This post processing method could be implemented in real time using the same logic if future tests were conducted (Donald L. Simon, 2010).

4 RESULTS

4.1 Expander performance

A total of 119 steady state points were obtained in the trial, and of these 60 were deemed valid to be used in examining performance (section 5.2). Figure 4 shows the isentropic efficiency of the expander. As there was no provision to control RPM, the next most relevant metric for comparison is with the heat extracted by the working fluid, Q_evap:

$$Q_{evap} = \dot{m}_r\left(h_{evap,ex} - h_{evap,su}\right) \quad (4)$$

Where $\dot{m}_r$ is the refrigerant mass flow rate.

Work by Lemort et al. shows the adiabatic definition of the isentropic efficiency cannot be used in the case of a scroll expander, as it exchanges a non-negligible amount of heat with the environment even when insulated (Lemort, Quoilin, Cuevas, & Lebrun, 2009). The isentropic efficiency is therefore calculated by:

$$\varepsilon_s = \frac{\dot{W}_{gen}}{\dot{m}_r(h_{su} - h_{ex,s})} \quad (5)$$

Where $\dot{W}_{gen}$ is the measured generated power, h_{su} is the enthalpy at the supply and $h_{ex,s}$ the isentropic enthalpy at the exhaust.

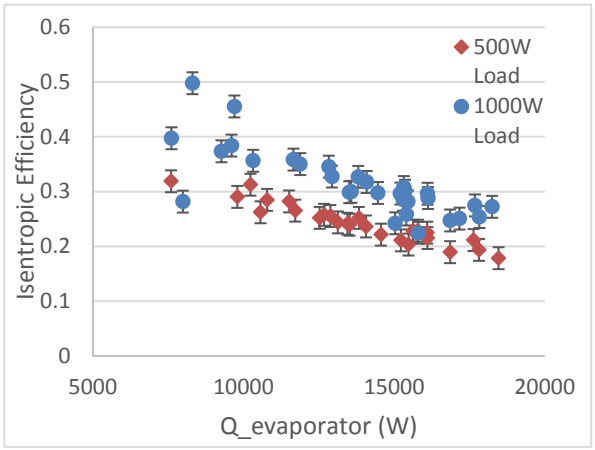

Figure 4 - Isentropic efficiency vs Available heat (Q_evaporator, (W)) created by trial input range

The maximum isentropic efficiency achieved was 40 ± 5%. This is comparatively low compared to scroll efficiencies achieved elsewhere which can reach 75% (Declaye et al., 2013). If rotational speed was able to be controlled, a curve with a maximum isentropic efficiency would be expected – however a monotonic decreasing function is evident from the data. One thermodynamic explanation is the fact superheating was not controlled in the test, rather it was observed as part of the system response to inputs. With the maximum pressure already reached, superheating reached up to 60 degrees in certain cases, representing a large efficiency loss.

Another source for the trend may be due to the effect of rotational speed. Figure 5 shows the same monotonic decrease with increased RPM. The expander is known to have suffered from bearing losses that most likely increased over time. A higher RPM increases the magnitude of these losses, decreasing isentropic efficiency.

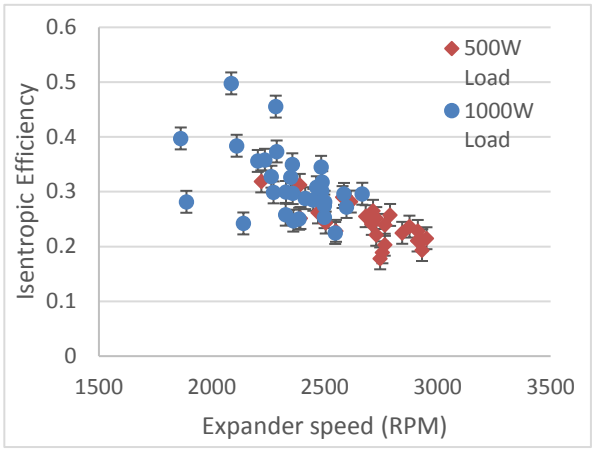

Figure 5 - Isentropic efficiency vs RPM

In contrast to efficiency, the measured power was a monotonically increasing function of the pressure ratio between inlet and outlet. Due to the measurement being taken from the generated power, it should be noted the value will be less than actual shaft work produced by the expander, due to mechanical/transmission losses and generator losses. The maximum work generated was 597 W. The increasing nature of this function is explained by the fact that the pressure ratio applied to the expander increases above the one corresponding to the built in volume ratio, and therefore a part of the expansion takes place at constant volume. The relative contribution of this expansion increases with the pressure ratio, thus decreasing isentropic efficiency but increasing the overall work production of the system (Declaye et al., 2013).

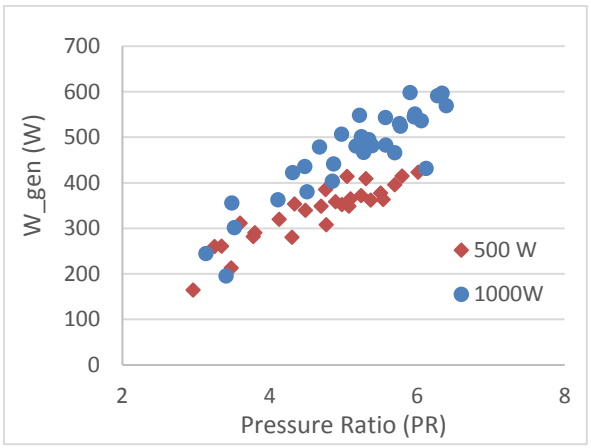

Figure 6 - Generated power vs Pressure ratio

4.2 Cycle performance

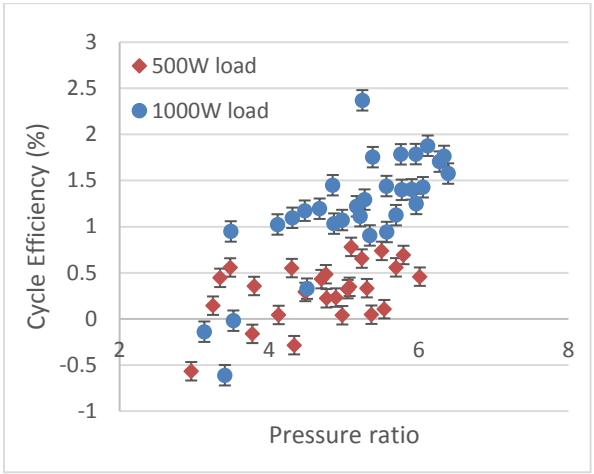

Figure 7 - Cycle efficiency as a function of the pressure ratio

Figure 5 shows the effect of the pressure ratio imposed on the expander on the cycle efficiency of the ORC system. The cycle efficiency is defined as:

$$\eta_{cycle} = \frac{\dot{W}_{net}}{Q_{evap}} = \frac{(\dot{W}_{gen} - (\dot{W}_{wf,pump} + \dot{W}_{tf,pump}))}{Q_{evap}} \quad (6)$$

Similarly to the shaft power, the results weakly suggest the cycle efficiency is a monotonically increasing function of the pressure ratio, with a maximum of 1.9 ± .1% The low absolute value is exacerbated by the power consumption of the transfer fluid pump. Previous works on this system incorrectly assumed this to be negligible, whilst in reality it was found to consume up to 20% of the maximum generated power, causing a number of negative efficiency operating

points. Ignoring the oil loop, the maximum efficiency was 2.9 ± .2%

4.3 Theoretical Comparison

The cycle was modelled using basic Rankine cycle principles and relationships, with R245fa as the working fluid, and forgoing a heat transfer pump.

Using the resulting states of the trials, and assuming an isentropic efficiency of 75% for the expander, the maximum cycle efficiency was calculated to be 11.2%, indicating the system was hampered in its operation to approximately 30% of its potential. Causes for this such as the component wear and eventual failure are detailed in section 5.1.

4.4 DVR Tests

The dimensionless volume ratio tests did not yield sufficient data to draw solid conclusions. Figure 8 allows some insight into the effect the DVR has on the potential operating range of the system, by examining the mass flow rate required at the highest achievable pressure ratios. This indicates the range drops off sharply with decreasing DVR. To properly ascertain the effect of the DVR on the system, a set of steady state operating points using an expander is required.

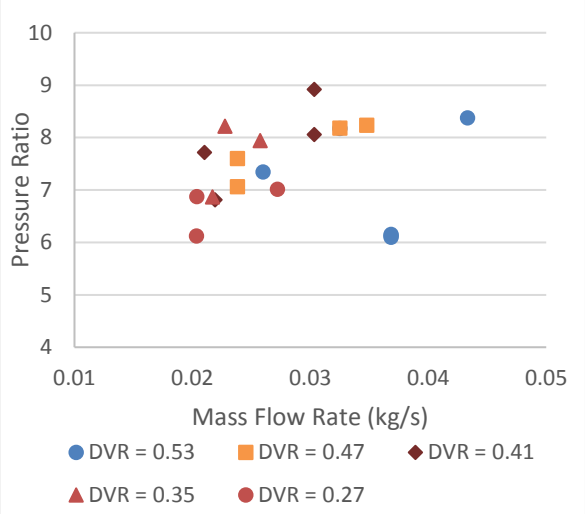

Figure 9 - DVR results indicating potential operating range

5 OBSERVATIONS

5.1 Component failures

During the initial trials, it was noted that the expander began to make sounds indicating bearing failure. Eventually the expander became inoperable, and upon disassembly it was found all 5 bearings were without lubricant. Two had resistance to rotation and the rear main shaft bearing was completely seized, with the shaft rotating on the inner race. Metal flakes were found in the housing, and found in the condensed refrigerant upon draining, suggesting transport down the system. The bearings were dissected and determined to be the most likely source of these flakes.

The cause of the bearing failure is postulated to be seal incompatibility with the working fluid. Both nitrile rubber and PTFE seals were affected by the fluid, with PTFE shredding and nitrile rubber expanding. An unidentified oily residue was also found to be coating the inside of the buffer tank, which obscured the optical level sensors, and in the refrigerant drained from the evaporator. This may be the bearing lubricant, as other sources of oil infiltration into the

Figure 8 - Left: Example of metal flakes found in bearing housing. Right: A section of the outer race of the seized bearing.

system were ruled unlikely upon inspection.

Pinhole leaks in the evaporator exit flange weld were identified during operation mid-way through the tests. The system was initially charged with 9.26 kg, with only 7.9 kg recovered a month later, meaning a substantial loss of 1.36 kg (roughly 15% of initial charge). At the time, to continue testing, this was addressed using a wicking grade Loctite product with thermal stability up to 130ºC. Initially this was successful, however by the conclusion of the DVR tests it had reopened, with a loss of 500 g.

All these issues will have had an effect on system performance, and their time dependent nature introduces a large amount of uncertainty into any results obtained in the trials. Rather, these can still be viewed to present trends of relationships between variables rather than using values to infer design decisions.

5.2 Potential condensation in expander

Before component failure, 119 steady state points were recorded for the scroll tests. Upon investigation of the results, it was found that in 50% of the points, entropy at the exhaust was lower than the inlet by a significant margin. While heat loss to the surroundings will lower entropy, it is unlikely to affect it to this degree. Using REFPROP to determine the states of the constituent fluids in the M1 mix at these points, showed in 65% of these cases 365mfc was in a sub-cooled state. This suggests that the 365mfc may have been condensing in the expander, and as such not undergoing an expansion process and allowing for calculation of common efficiencies. The remaining 50% of steady state points were used, with caution where there was only a small difference between the entry and exhaust entropies.

5.3 Component incompatibility

The system was initially designed with R245fa as the intended working fluid, with the expander claiming fluid

compatibility. However due to supply restrictions in NZ, pure R245fa was unobtainable, and M1 was the next best alternative. Additionally zeotropic fluids theoretically have an improved performance over their pure constituents, combining preferable fluid properties. In this system the practical shortcomings of using a mixture have been demonstrated, with the unknown expansion behaviour and chemical incompatibility with system components. It is recommended that a pure fluid be used in the first trial of a test system, to remove the uncertainties.

Due to incorrect specification from a previous team, the variable area flow meter had a poorly suited resolution for its analogue reading. The scale started at 0.95 L/min, with only half a division between that and the next increment at 2.00, then normal divisions up to 9.5. With the maximum flow rate achieved by the fluid pump being 2.5 L/min, this made reading the flow meter difficult. Furthermore, at lower frequencies, the pressure pulses inherent in a positive displacement pump became more prevalent, causing further difficulty in reading. This could have been avoided by either selecting an appropriate scale when ordering the flow meter, purchasing the digital output package and integrating the result with a high sample rate, or by using a Coriolis flow meter.

The generator is designed to operate at 3000 RPM to provide grid compliant power. It attempts to achieve and regulate this using internally switched resistive loads cooled by its fan. This makes the generator unfit for purpose, with generated power being a crucial metric of the system. During operation, switching the resistance of the light bulb bank with all other inputs constant caused an instant increase in measured power of roughly 50W, suggesting the generator could be interfering with the results. Instead, in systems such as these it is common practice to measure the shaft work of the expander using a torque transducer, and control the speed of the generator with a wider range of resistive loads (Lemort et al., 2009). With such a setup, it is possible to control the rotational speed of the expander, so as to evaluate performance at different speeds.

5.4 Uncertainties, measurement error

Table 4: Error of measurement devices as specified by their respective manufacturers.

Component	Error
Thermocouples	K-type ±0.5°C
Pressure transducers	LP ±14 kPa, HP ±28 kPa
Clamp meter	2.5% of measured value
Water flow meter	1.5% of measured value
Variable area flow meter	10% of measured value (estimate)

5.5 Analytical sources of error

The property information contained in the REFPROP database contains an unknown level of inaccuracy for some fluids (DiPippo & Moya, 2013). This is applicable to the M1 mixture used as the mixing parameters were estimated and these may not reflect reality as postulated in section 5.2.

5.6 Error analysis on efficiency calculation

An error propagation analysis including both the measurement error and potential heat loss indicates that the total accounted relative error of the measured net thermal efficiency value is ±1.3%. A large portion of this error (±0.8%) is attributable to low accuracy of the mass flow rate readings, outlined previously.

6 CONCLUSION

This paper presents experimental results from running a 1 kW ORC system using HFC-M1 refrigerant as a working fluid under a wide range of operating conditions, to investigate system performance.

Trials began well, but a host of operating issues hampered performance, and culminated in insufficient data quality for clear conclusions. For the periods least impacted by these faults, a maximum power of 567W was produced, and maximum isentropic and cycle efficiencies of 40% and 1.9% were achieved, respectively. Decreasing the volume ratio of refrigerant in the system sharply decreased the operating range, but further conclusions as to its impact cannot be drawn at this stage.

A comparative study performed between the system actual performance and the theoretical performance found operational issues limited the system to roughly 30% of its potential.

Critiques of components and working fluid derived from experiences in operating the system, coupled with general trends produced by the results, provide useful consideration for designs of future systems.

7 ACKNOWLEDGEMENTS

The author would like to thank the ORC research team at the University of Canterbury for their helpful feedback and ideas. The author would also like to thank Dr. Susan Krumdieck of the University of Canterbury for her continued support and direction.

8 REFERENCES

Capstone, T. C. (2006). *Technical Reference Capstone Model C30*

Declaye, S., Quoilin, S., Guillaume, L., & Lemort, V. (2013). Experimental study on an open-drive scroll expander integrated into an ORC (Organic Rankine Cycle) system with R245fa as working fluid. *Energy*, *55*, 173-183. doi: http://dx.doi.org/10.1016/j.energy.2013.04.003

DiPippo, R., & Moya, P. (2013). Las Pailas geothermal binary power plant, Rincón de la Vieja, Costa Rica: Performance assessment of plant and alternatives. *Geothermics*, *48*(0), 1-15. doi: http://dx.doi.org/10.1016/j.geothermics.2013.03.006

Donald L. Simon, J. S. L. (2010). *A Data Filter for Identifying Steady-State Operating Points in Engine Flight Data for Condition Monitoring Applications*. Glenn Research Center, Cleveland, Ohio. NASA/TM.

Engel, F. (2013). *Experiemental Investigation and Derived Considerations for the Scale-Up of a Finned-Tube Heat Exchanger for Exhause Gas Heat Recovery.* (Master's Thesis). Hamburg University of Technology.

Lemmon, E. W., McLinden, M.O., Huber, M.L. (2013). REFPROP-Reference Fluid Thermodynamic and Transport Properties (Version 9.0): NIST NSRDS.

Lemort, V., Quoilin, S., Cuevas, C., & Lebrun, J. (2009). Testing and modeling a scroll expander integrated into an Organic Rankine Cycle. *Applied Thermal Engineering*, *29*(14–15), 3094-3102. doi: http://dx.doi.org/10.1016/j.applthermaleng.2009.04.013

Li, T., Zhu, J., Fu, W., & Hu, K. (2015). Experimental comparison of R245fa and R245fa/R601a for organic Rankine cycle using scroll expander. *International Journal of Energy Research*, *39*(2), 202-214. doi: 10.1002/er.3228

Meyer, D., Wong, C., Engel, F., & Krumdieck, S. (2013). *Design and Build of a 1 Kilowatt Organic Rankine Cycle Power Generator*. Paper presented at the Paper presented at the 35th New Zealand Geothermal Workshop, Rotorua, New Zealand. .

Southon, M., & Krumdieck, S. (2014). *Commissioning, Initial Testing and Results From an Experimental One Kilowatt Organic Rankine Cycle.* Paper presented at the Proceedings 36th New Zealand Geothermal Workshop.